JOURNAL OF MATERIALS SCIENCE **34** (1999) 2695–2702

Cavitation behaviour in fine grain 3Y-TZP during tensile and compressive superplastic flow

Z. C. WANG, N. RIDLEY and T. J. DAVIES
University of Manchester and UMIST, Materials Science Centre, Grosvenor Street, Manchester M1 7HS, UK

Studies of cavitation in Y-TZP during superplastic flow have been made for both tensile and compressive deformation conditions. It was observed that the morphologies of cavities near the fracture faces of tensile specimens varied markedly with testing conditions and in most cases differed from those near the gauge heads. Two quite different forms of cavitation behaviour were observed leading to high and low strains to failure, respectively. For optimum conditions of superplastic flow, of high temperature/low strain rate (low stress), when large elongations were observed, cavities were either spherical or elongated parallel to the tensile axis. Those near the fracture face interlinked in a plastic (necking) mode to give transverse cavities and subsequent failure. At high strain rate/low temperature (high stress), transverse intergranular cracking played a dominant role in failure at low elongations. For intermediate conditions of temperature/strain rate, elongated cavities developed parallel to the tensile axis, but near the fracture face these usually interlinked by transverse cracking. These conditions were associated with intermediate elongations to failure. For the assessment of cavity growth mechanisms, artificial pores were introduced into fine grain Y-TZP specimens and changes in their shape and size during tensile or compressive deformation were investigated. Results show that the change of pore volume, in the superplastic regime, is controlled by plastic deformation of the matrix and can be described by the relationship of $dR/d\varepsilon = \eta R$, where ε is the true strain, η the cavity growth rate parameter and R is the radius of the pore.

1. Introduction

Most fine grain pseudo-single phase and microduplex materials undergo cavitation during superplastic flow. While the phenomenon has been widely studied in metals, the cavitation behaviour of ceramic materials has been studied to a lesser extent and has also resulted in conflicting observations [1–4].

In superplastic metals, elongated cavities or stringers usually develop parallel to the tensile axis. The extent of cavitation may increase or decrease with increasing strain rate or temperature, depending on materials, testing conditions and microstructural stability [5]. Generally in ceramics, cavities/cracks propagate in a direction perpendicular to the axis of applied tensile stress and interlink to cause failure at relatively small strains, as in the case of fine grain aluminas. However, in superplastic Y-TZP (yttria-stabilized tetragonal zirconia polycrystals), a cavitation mode similar to that in metallic systems exists where cavities grow and align parallel to the tensile axis. The elongation to failure in Y-TZP is significantly higher than in other ceramic systems as a consequence. Stringers of cavities lying along the tensile axis have only been reported for large elongations [6] and/or when significant amounts of grain boundary glassy phase were present in superplastic ceramic systems [7]. The extent of cavitation has been observed to increase with increasing strain rate for alumina, Y-TZP and zirconia-alumina composites [4, 8, 9], but the cavity area fraction for a Y-TZP was observed to peak at the optimum strain rate for which specimens showed the largest elongation [3, 6].

In our earlier reports [10, 11], the superplastic behaviours of Y-TZP and doped aluminas were related to the 'metallic' character of the material. It was proposed that the metallic behaviour was a consequence of preferred bonding arrangements that could be explained using an electron-theory approach [10]. The present work deals with cavitation and changes in the morphology of pores/cavities during tensile or compressive superplastic deformation for a Y-TZP. To achieve the objective of studying changes in pore/cavity shape, size and orientation, artificial pores were also introduced into specimens and their behaviours were monitored during tensile or compressive deformation.

For ease of discussion in later sections, the relationship between strain rate ($\dot{\varepsilon}$) and stress (σ) for superplastic creep deformation is adopted as:

$$\dot{\varepsilon} = \frac{ADbG}{kT}\left(\frac{b}{d}\right)^{p}\left(\frac{\sigma}{G}\right)^{1/m} \quad (1)$$

where A is a constant, D is the diffusion coefficient, G is the shear modulus, b is the Burgers vector, k is Boltzmann's constant, T is the temperature in degrees Kelvin, p is the grain size exponent and m is the strain rate sensitivity exponent.

2. Experimental

The starting material was a 3mol%Y_2O_3 stabilized zirconia powder, grade HSY-3U supplied by Mandoval Zirconia Sales (UK) Ltd. The composition (wt %) of the TZP was 5.4Y_2O_3-0.11SiO_2-0.12TiO_2-0.25Al_2O_3-0.003Fe_2O_3-0.02Na_2O-0.06CaO and balance $ZrO_2 + HfO_2$. The average particle size was 0.2 μm. Tensile specimens were prepared by slip-casting to net-shape using a procedure previously developed by the authors [12]. In order to introduce artificial pores, the slurries were slightly shaken before casting and consequently some bubbles with diameters ranging from 1 to 50 μm were formed in the surfaces of the specimens. The green bodies were densified by CIPing (cold isostatic pressing) at 280 MPa, followed by pressureless sintering at 1723 K for 1 hour. The sintered materials contained 100% tetragonal phase, had densities greater than 98% and a uniformly distributed equiaxed grain size of 0.33 μm [12]. The specimens for compressive tests were cut from the gauge length of tensile specimens and had dimensions of $3.5 \times 4.0 \times 7.0\,mm^3$. Both tensile and compressive tests were performed in the strain rate range 5×10^{-5} to 2×10^{-2} s^{-1} and at temperatures of 1473 to 1873 K.

The uniaxial tensile testing procedures have been described previously [10, 11]; a similar experimental set-up was also used for compressive testing in which specimens were placed between two SiC platens and deformed at constant strain rates. True stress, σ, and true strain, ε, were defined, respectively, as:

$$\sigma = \frac{Pl}{l_0 A_0} \quad \varepsilon = \ln\left(\frac{l}{l_0}\right) \tag{2}$$

where P is the load, l and A are gauge length and cross-section area, respectively; the subscript '0' denotes the original dimensions. Engineering strain, e, for both tensile and compressive tests is defined as $e = \{(l - l_0)/l_0\} \times 100\%$. The absolute values of both true strain (ε) and engineering strain (e) for compression tests are used in discussion.

The growth of artificial pores (formed as described above) is a procedure which can be used to simulate the growth of single cavities in which the effects of cavity coalescence, continuous cavity nucleation and heterogenous cavity distribution can be avoided. For each specimen in either tensile or compressive testing, deformation was interrupted at various strains and changes in pore morphologies were recorded and examined using scanning electron microscopy (SEM) techniques. Pores with an initial radius $r_0 > 10$ μm were studied in tensile deformation and those with $r_0 > 30$ μm were studied in compression. Morphology changes in about 10 pores distributed over an area of $\sim$2 mm^2 in either tensile or compressive specimen surfaces were investigated.

3. Results

3.1. General superplastic behaviour

The 3Y-TZP shows superplastic behaviour at temperatures above 1473 K, under both tension and compression at strain rates around 10^{-4} s^{-1}. An apparent superplastic steady state observed at 1573 K at an applied strain rate of 1×10^{-4} s^{-1} was probably the result of a balance between grain growth (strain hardening) and cavitation (strain softening). Under other testing conditions within the experimental range, flow stress was observed to increase continuously with strain. The largest elongation to failure of 480% was observed at 1823 K and a strain rate of 1×10^{-4} s^{-1}.

The material had a uniform grain size and during superplastic tensile deformation there was no obvious external localized necking [13]. However, if local strain (the cross-sectional area strain, $\ln(A_0/A)$), uncorrected for cavitation, is plotted against normalized positions along the gauge length (defined as the fractional distance from one end of the gauge length when the whole gauge length is taken as unity), a gradual increase in the amount of local strain is seen to occur in the vicinity of the final fracture region in specimens with elongations greater than 300%, i.e. for those specimens tested at strain rates lower than 5×10^{-3} s^{-1} and at temperatures higher than 1673 K. For specimens with lower elongations, e.g. when deformed at higher strain rates or lower temperatures, there were no obvious local strain regions and the strain was uniformly distributed along the gauge length, as seen in Figs 1a and 2a. These observations are consistent with those of Nieh and Wadsworth [6] and Schissler *et al.* [3].

The strain rate sensitivity value, m, for the TZP for temperatures from 1573 to 1873 K lay in the range 0.44–0.54, as determined by cross-head velocity change tests [13]. This, together with the manufacturers compositional data, places the TZP used in the present work into the "low purity" category according to the

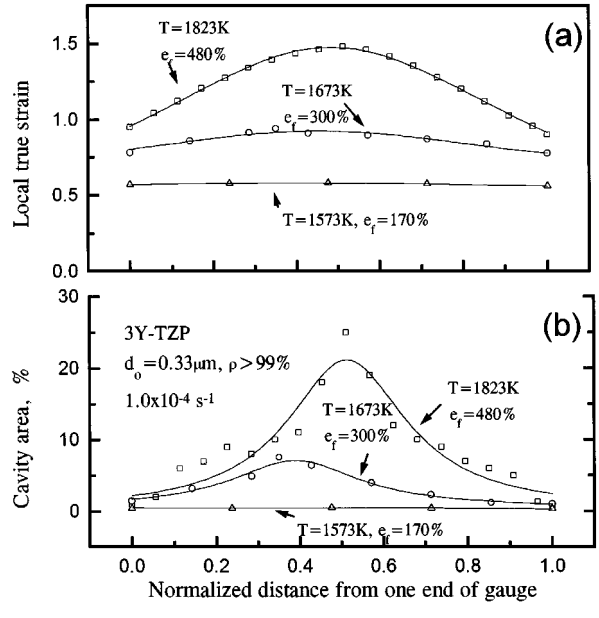

Figure 1 (a) Local true strain and (b) cavity area fraction as a function of normalized position in the gauge length for Y-TZP at a strain rate of 1.0×10^{-4} s^{-1} when strained to failure at various temperatures.

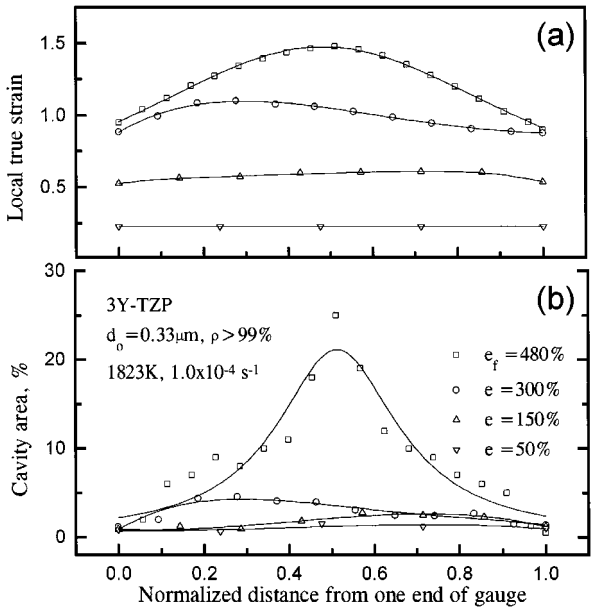

Figure 2 (a) Local true strain and (b) cavity area fraction as a function of normalized position in the gauge length, for Y-TZP at 1823 K and 1.0×10^{-4} s^{-1} after straining to various elongations.

Figure 3 TEM micrograph of a specimen tested at 1823 K, 2×10^{-2} s^{-1}, showing intergranular cracks seen as white features at mid-section of the photograph; arrows indicate tensile direction.

conclusions of Carry [14] and Langdon [15]. The activation energy for superplastic flow was determined to be 592 ± 45 kJ mol^{-1} for the stress range of 5–20 MPa, and the grain size exponent, p in Equation 1, was 1.65–1.71 [13].

3.2. Cavity development and distribution during tensile deformation

Generally, for all deformation conditions, cavities were seen to nucleate at grain boundary triple points. For some test conditions, intergranular cracks running perpendicular to the tensile stress axis were observed. Fig. 3 is a TEM micrograph of a specimen tested at a strain rate of 2×10^{-2} s^{-1} and at 1823 K with $e_f \sim$ 150%, and shows features which are believed to illustrate the early stages of intergranular cracking.

Although deformation along the gauge length was relatively uniform, the cavity distribution was nonuniform, particularly for specimens with large elongations to failure. Fig. 1b shows the distribution of cavity area percent at normalized positions along the gauge length for specimens pulled to failure at various temperatures and at a strain rate of 1×10^{-4} s^{-1}. It is seen that the extent of cavitation near the fracture face can be five times as high as that near the gauge head; the lower the total elongation to failure, the more uniform is the distribution of cavities in the gauge length.

For specimens tested at the same temperature and strain rate, but to various elongations, the distribution of cavities in the gauge length is shown in Fig. 2b. When total elongations were less than 300%, the maximum local cavity area fraction was only ∼5% and was fairly uniformly distributed along the gauge length. However, at an elongation to failure of 480%, as much as 25% cavitation was observed near the fracture face.

The morphologies of cavities near the fracture faces of tensile specimens varied markedly with testing conditions and in most cases differed from those near the gauge head, as can be seen in Figs 4 and 5. Two quite different forms of cavitation behaviour were observed leading, respectively, to high and low strains to failure. At high strain rate and low temperature (high stress), e.g. 1723 K; 2×10^{-2} s^{-1}, transverse intergranular cracking played a dominant role in failure, giving low elongations (∼20%). Under optimum conditions of superplastic flow of high temperature and low strain rate (low stress), i.e. 1823 K; 10^{-4} s^{-1}, cavities were either spherical or elongated parallel to tensile axis (Fig. 4a). At high strains (∼500% elongation) those near the fracture face interlinked in a plastic (necking) mode, to form transverse cavities (Fig. 4b and c). For intermediate conditions of temperature/strain rate, e.g. 1823 K; 2×10^{-2} s^{-1}, elongated cavities formed along the gauge length, but failure occurred by transverse cracking. This latter behaviour led to intermediate elongations to failure, e.g. ∼150%. A further example of elongated or roughly spherical cavities near the gauge head is seen in specimens tested at a strain rate of 5×10^{-5} s^{-1} and a temperature of 1723 K. Ultimate failure at a relatively low flow stress occurred by the link-up of these cavities in a transverse direction (Fig. 5); these test conditions produced elongations of ∼300%. The different mode of cavitation and failure are illustrated in Fig. 6.

3.3. Change in shape and size of artificial pores during deformation

Fig. 7 shows pore shape change during tensile and compressive deformation; it is seen that pores become longer in the tensile direction and narrower in the compressive direction as deformation proceeds.

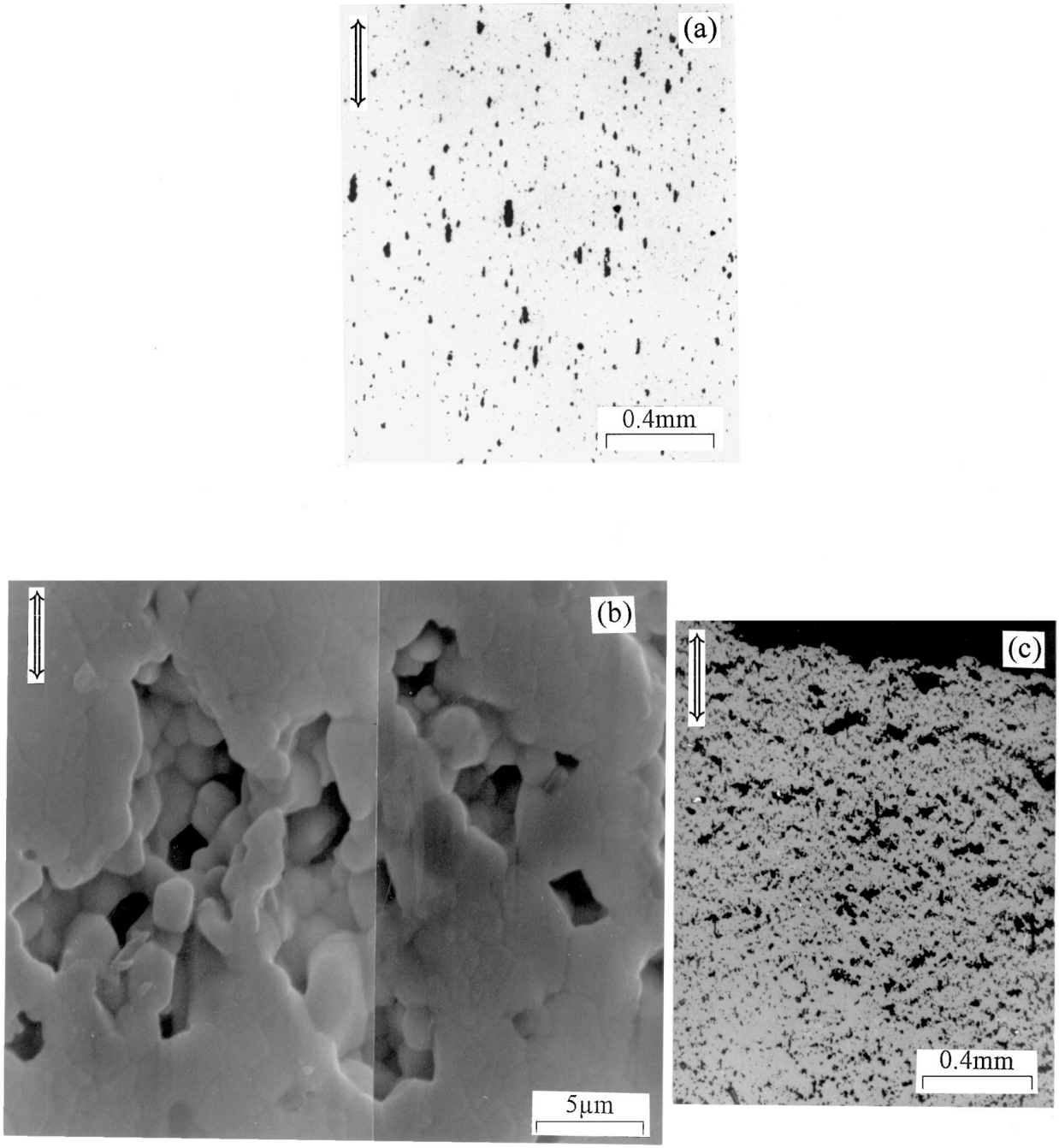

Figure 4 Shows (a) spherical and elongated cavities near gauge head, (b) the interlinkage of elongated cavities near the fracture face by necking, (c) same as (b) but at a lower magnification. TZP, $\dot{\varepsilon} = 1 \times 10^{-4}$ s^{-1}, $T = 1823$ K; arrows indicate the tensile stress.

For quantitative analyses, the artificial pores were assumed to be ellipsoidal in shape. It has been shown that this geometrical model was consistent with experimental observations particularly when elongations were less than 200% ($\varepsilon < 1.1$) [13]. The radius of a sphere having the same volume was used as the equivalent radius, and changes with strain under various conditions are plotted in Fig. 8a. The data points represent the mean values for ten pores and the error bars are the two extremes. It is seen from Fig. 8a that the equivalent spherical pore radius, and thus the volume of the pores, increases with increasing tensile strain. Correspondingly, for compressive deformation, artificial pores close up along the compressive axis and expand in the transverse direction.

4. Discussion

4.1. Cavity nucleation

Grain boundary triple points are frequently reported as preferred sites for cavity nucleation during superplastic deformation of ceramic materials, e.g. the TZPs without glassy phase [3, 9] and glass ceramics containing glass pockets in triple points [16]. Although the present material contains impurities, no glass pockets were observed by both high resolution and dark field TEM techniques [13]. It is believed that cavities are nucleated at stress concentrations at grain boundaries [5]. Evidence for these regions of stress concentration is presented in Fig. 9, which shows a strain field expanding from point B to point A by the pile-up of dislocations in the grain boundary. In this test, the compressive stress (normal

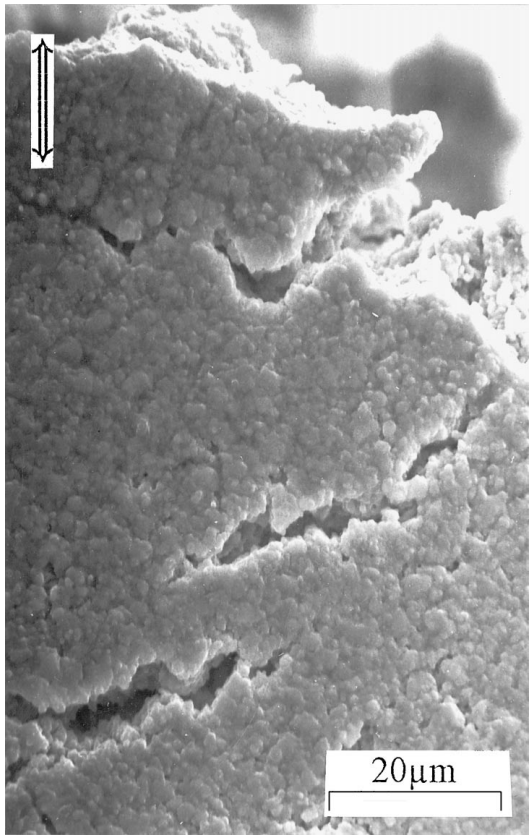

Figure 5 Shows cracks transverse to tensile axis near the fracture face for the TZP tested at $\dot{\varepsilon} = 5 \times 10^{-5}$ s^{-1} and $T = 1723$ K; arrows indicate the tensile stress.

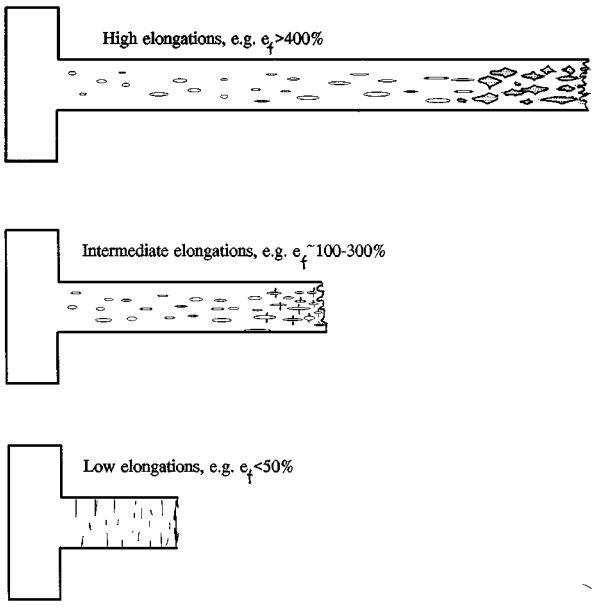

Figure 6 Schematic illustration of the relationship between cavitation mode and elongations to failure in superplastic materials.

to the plane of the page) was maintained during cooling. The spacing between the dislocations is observed to decrease from ~19 nm near point A to ~7 nm near point B.

The important role of grain boundary dislocations during superplastic deformation has been previously discussed [17–19], and many of the phenomena associated with superplastic flow have been successfully explained on the basis of movement and reactions of grain boundary dislocations. It has been predicted that cavities can be generated at grain boundaries if the local stress exceeds the interface rupture strength or if vacancies can coalesce into a size greater than a critical nucleation size [19–21]. In both cases, stress concentration plays an important role. The main cause of stress concentrations in ceramic materials during deformation at high temperatures is as a result of grain boundary sliding (gbs) [20]; the relaxation of these (elastic) stress concentrations is temperature, strain rate and microstructural dependent. For certain testing and/or microstructural conditions, the stress concentration cannot be relaxed rapidly enough, by either dislocation or diffusion processes, and cavities will nucleate.

Intergranular cracks were frequently observed in specimens pulled at strain rates higher than 1.0×10^{-2} s^{-1} and at temperatures lower than 1823 K. Since stress concentration factors caused by grain boundary displacements in ceramics are typically greater than 2 [20], local stresses at grain boundaries can be higher than 100 MPa and, for some orientations, this may exceed the grain boundary cohesive strength [22] resulting in grain boundary cracks. When the present material was tested under optimum superplastic conditions, no cracking was seen.

No large cavities were formed during compression testing, although small cavities which had nucleated at triple points were observed. Samples did not fail by cavitation or cracking during compressive deformation. Due to the testing procedure, the applied stress increased rapidly in the later stages of deformation because of end friction. Although the mechanism of cavity nucleation should be the same for tension and compression, cavity growth only occurs where a tensile stress exists [23].

4.2. The role of cavitation in superplastic deformation

The transverse cavities/cracks observed near the fracture face may be the result of a combined consequence of a tensile stress, grain boundary sliding and a critical grain size condition. Yoshizawa and Sakuma [8] have suggested that there is a critical grain size for superplasticity (either initial or developed during deformation) which is a function of temperature and strain rate. According to this concept, when the grain size exceeds a critical value, cavities/cracks propagate in transverse direction because the accommodation processes are not rapid enough, leading to rapid failure [20, 21]. Some specimens failed soon after the stress reached a peak value; this peak stress could correspond to the critical grain size, at which transverse cavities/cracks develop rapidly. Fig. 2 shows that within a range of testing conditions, little cavitation is observed until 300% elongation, which suggests that most of the cavities develop during the later stages of deformation. The grain size at failure may be used as an upperbound value of the critical grain size, d_c. For TZP in the present work, the value is $d_c = 1.2$–1.5 μm, which is reasonably comparable with $d_c = 1.2$–2.5 μm for pure or MgO-doped alumina [8], for similar testing conditions to those used

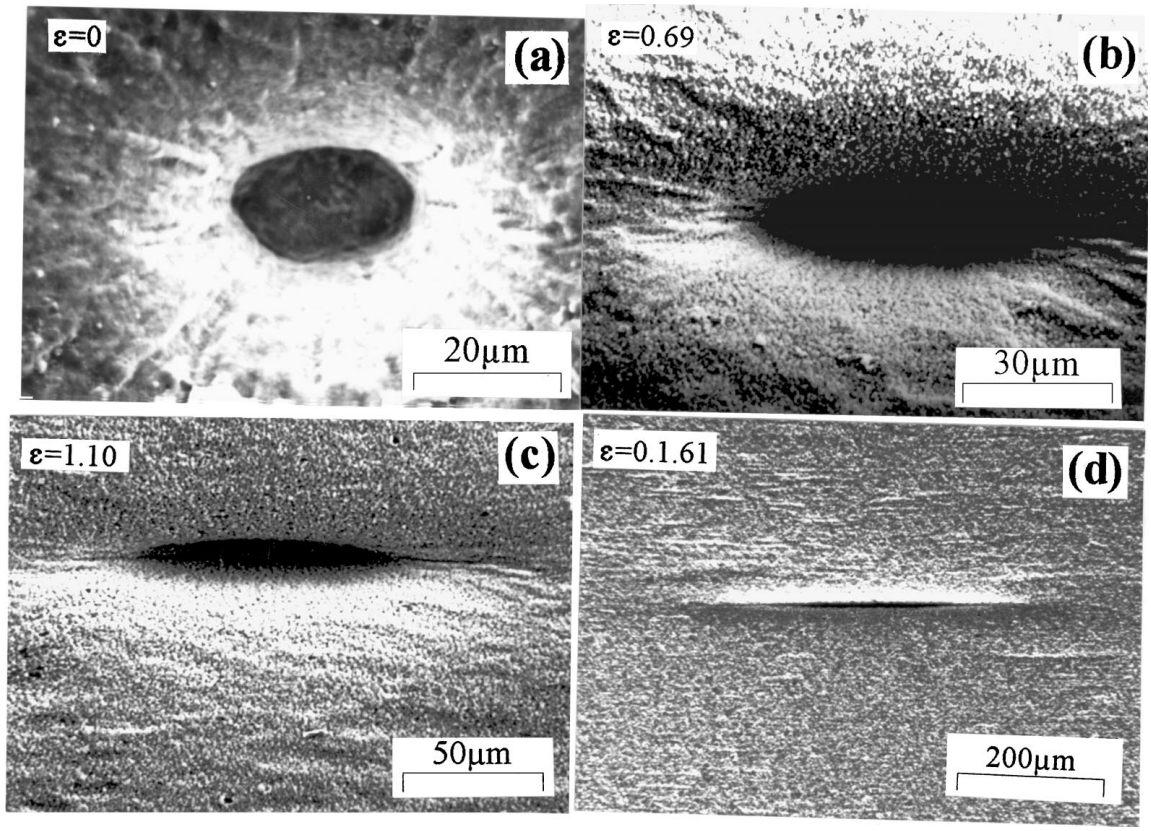

Figure 7 Change of pore morphology of TZP during tensile deformation, $T = 1823$ K and $\dot{\varepsilon} = 1.0 \times 10^{-4}$ s^{-1}, loading direction horizontal.

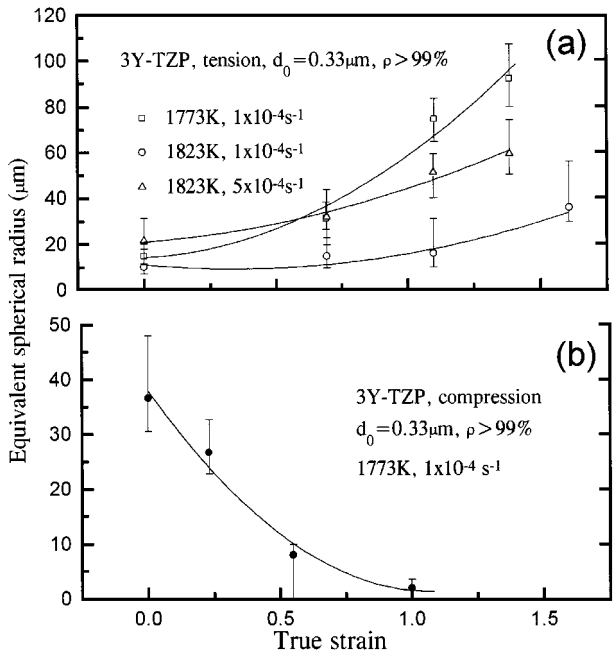

Figure 8 Changes in pore radius with superplastic strain for 3Y-TZP under (a) various tensile test conditions and (b) under compression at 1773 K and 1.0×10^{-4} s^{-1}.

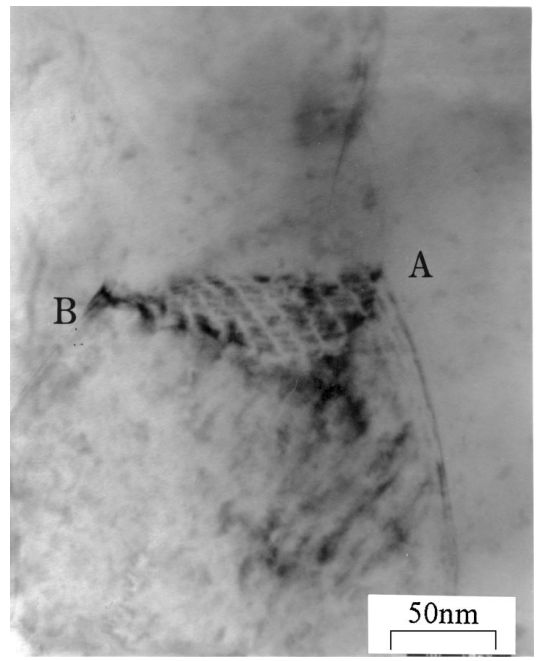

Figure 9 TEM micrograph shows strain field associated with grain boundary dislocations in Y-TZP. Dislocation spacing increases from A (19 nm) to B (7 nm) and more severe strains are seen near B. Compressive testing at 1773 K, 8.0×10^{-4} s^{-1}; stress (∼100 MPa) was maintained during cooling. Stress normal to the plane of paper.

in the present work. This critical grain size is in accord with the general view that for superplastic ceramic materials the grain size should be ∼1 μm or smaller [24].

Transverse cavities as seen in Fig. 4c are mainly caused by coalescence of elongated cavities through necking. This type of cavitation has been observed most frequently in Y-TZP during superplastic deformation [3, 7, 10, 25]. The spherical and elongated cavities observed near the gauge head in the Y-TZP specimens are very similar to those observed in metallic materials [5]. Spherical cavities in metals elongate by a plasticity-controlled mechanism that dominates cavity growth after an initial rounding of cavities by diffusional processes. The transverse cracks seen in

Fig. 5 are mainly formed by the propagation of single cavities/cracks, although coalescence with other cavities/cracks will certainly accelerate their growth.

The spherical and elongated cavities as well as the transverse cavities observed in TZP are in sharp contrast to cavitation (or cracking) in 'normal' superplastic ceramics [8], such as Al_2O_3, where cracks propagate perpendicular to the tensile axis. To account for the different behaviour in Y-TZP, Davies *et al.* [10] have proposed that the observed plasticity may be explained by consideration of the energies of d-state electrons of dopants, e.g. yttria in zirconia for Y-TZP. These dopants contribute a 'metallic' character to the bonding and lead to development of large extensions and elongated cavities under certain testing conditions. The 'metallization' is primarily related to dopant segregation at high angle grain boundaries. Direct evidence for yttria and copper oxide segregation at TZP grain boundaries has been provided by X-ray photoelectron spectroscopy [26] and EDX [11]. These localized changes in composition and stoichiometry and the associated 'metallic' behaviour can provide mechanisms for resisting nucleation and propagation of transverse cracks or cavities [10].

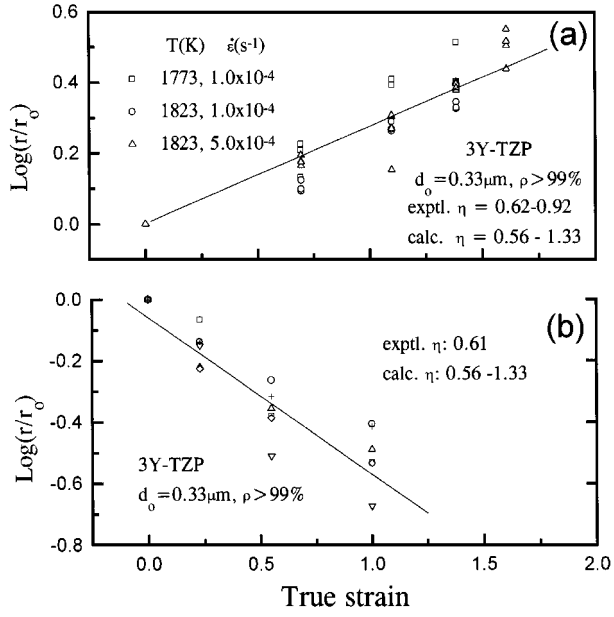

Figure 10 Variation of the relative radii of artificial pores with true strain for 3Y-TZP (a) in tension and (b) under compression.

4.3. Mechanisms of cavity growth during deformation

Three mechanisms have been proposed for cavity growth during superplastic deformation, including diffusion controlled growth [27], plasticity controlled growth [28] and superplasticity diffusion growth [29]. It has been demonstrated that cavity growth in metals is controlled primarily by plastic deformation of the matrix rather than by diffusion mechanisms, although the latter may be important during the very early stages of void growth [30], e.g. for very small cavities. Because insufficient diffusion data are available for TZP, it is impossible to quantitatively evaluate the contribution of diffusional mechanisms to cavitation. Alternatively however, if the cavity growth is governed by plastic deformation of the matrix material, the growth rate of a cavity may be expressed in the form of Equation 3 [28, 30, 31].

$$\mathrm{d}R/\mathrm{d}\varepsilon = \eta R \tag{3}$$

where R is the radius of cavity and η is the cavity growth rate parameter. Integrating Equation 3 gives $\ln(R/R_0) = \eta\varepsilon$ (where R_0 is the initial value of the cavity radius), from which η may be evaluated experimentally. From theoretical considerations, Pilling and Ridley [5, 30] express η as:

$$\eta = \left(\frac{1+m}{2m}\right)\sinh\left(\frac{2k}{3}\frac{2-m}{2+m}\right) \tag{4}$$

where k is a constant determined by the stress state and deformation mechanism. Under a uniaxial stress state, $k = 1$ when no gbs occurs (rigid grains) and $k = 2$ for deformation totally attributable to gbs [5]. The semi-logarithmic plots of relative pore radius, $\log(R/R_0)$, against true strain for tensile and compressive tests are presented in Fig. 10a and b, respectively. For the present work ($m = 0.5$), and the corresponding values of η are calculated to be $\eta_{\mathrm{rigid}} = 0.56$ and $\eta_{\mathrm{gbs}} = 1.32$, respectively.

It is seen from Fig. 10 that both pore growth rate during tensile deformation and pore closure rate in compression fall within the above two extreme values of η. This shows that the main growth mechanism for the artificial pores is plastic deformation accompanying the gbs. The experimental values are, however, closer to the rigid grain mechanism. If k is assumed to vary linearly with the contribution of gbs to the total deformation, only 30% of the elongation is attributable to the gbs mechanism; this value is lower than the generally predicted amount of 50–60%. For example, by assuming that 50% of the total elongation was the result of gbs, Guo and Ridley [32] obtained good agreement between measured and predicted η values for an aluminium alloy AA7475, deformed under both uniaxial and biaxial tensions. A recent assessment by Langdon [33] that superplastic deformation may be due totally to gbs is supported by the retention of equiaxed grains and the corresponding large elongations observed in the deformed specimens.

During compression tests, small pores ($r < 10\ \mu$m) grew during the early stages of deformation and then shrank, with further deformation, at the same rate as large pores. This is likely to be due to the inhomogeneity of compressive deformation leading to barrelling of the specimen and to the development of hoop (tensile) stresses in the surface, which stabilized the cavities in the tensile direction.

Previous work on the growth of artificially introduced cavities of radii 10–40 μm, during superplastic flow of alumina doped with CuO, were also consistent with a plasticity controlled growth mechanism [13].

5. Conclusions

Cavity growth and cavitation modes have been investigated in a Y-TZP under both tensile and compressive superplastic conditions. It has been observed that (a) the morphologies of cavities varied with testing conditions and (b) for a given testing condition cavities near the fracture face differed, in many cases, from those near the gauge heads. Two extreme forms of cavitation behaviour were observed leading, respectively, to high and low tensile elongations. Large elongations were obtained under optimum conditions for superplastic flow, when cavities were predominantly elongated parallel to the tensile axis; cavities near the fracture face linked up in a plastic (necking) mode, to form transverse cavities. At high strain rate and low temperature, transverse intergranular cracking played a substantial role in failure, leading to low elongations. For intermediate conditions of temperature and strain rate, elongated cavities formed and grew, but ultimate failure usually occurred by transverse cracking. This behaviour was associated with intermediate elongations to failure ($\sim$150%).

Quantitative studies show that change in the volume of artificial pores, under superplastic deformation conditions, is controlled by plastic deformation of the matrix material and can be described by the relationship of $\mathrm{d}R/\mathrm{d}\varepsilon = \eta R$, where ε is the true strain and η is a coefficient and R is the radius of the pore. For the present work, the η value is consistent with the relationship:

$$\eta = \left(\frac{1+m}{2m}\right)\sinh\left(\frac{2}{3}\frac{2-m}{2+m}\right)$$

where m is the strain rate sensitivity.

Acknowledgement

The work was supported by SERC under Grant No. GR/F 78866.

References

1. W.-J. KIM, J. WOLFENSTINE and O. D. SHERBY, *Acta Metall. Mater.* **39** (1991) 199.
2. Y. MA and T. G. LANGDON, *Mater. Sci. Eng.* **A168** (1993) 225.
3. D. J. SCHISSLER, A. H. CHOKSHI, T. G. NIEH and J. WADSWORTH, *Acta Metall. Mater.* **39** (1991) 3227.
4. J. YE, A. DOMINGUEZ-RODRIGUEZ and C. KAI, in "Progress in Advanced Materials and Mechanics (ICAM'96)," edited by Wang Tzuchiang and Tsu-wei Chou (Peking University Press, Beijing, 1996) p. 447.
5. J. PILLING and N. RIDLEY, "Superplasticity in Crystalline Solids" (The Institute of Metal, London, 1989).
6. T. G. NIEH and J. WADSWORTH, *Acta Metall. Mater.* **38** (1990) 1121.
7. K. KAJIHARA, Y. YOSHIZAWA and T. SAKUMA, *Scripta Metall. Mater.* **28** (1993) 559.
8. Y. YOSHIZAWA and T. SAKUMA, *Acta Metall. Mater.* **40** (1992) 2943.
9. S. PRIMDAHL, A. THÖLÉN and T. G. LANGDON, *ibid.* **43** (1995) 1211.
10. T. J. DAVIES, A. A. OGWU, N. RIDLEY and Z. C. WANG, *Acta Mater.* **44** (1996) 2373.
11. Z. C. WANG, T. J. DAVIES, N. RIDLEY and A. A. OGWU, *ibid.* **44** (1996) 4301.
12. Z. C. WANG, T. J. DAVIES and N. RIDLEY, *Scripta Metall. Mater.* **28** (1993) 301.
13. Z. C. WANG, PhD thesis, University of Manchester, Manchester, 1994.
14. C. CARRY, in "Superplasticity," edited by M. Kobayashi and F. Wakai (MRS, Pittsburgh, PA, 1989) p. 199.
15. T. G. LANGDON, *Mater. Sci. Eng.* **A166** (1993) 67.
16. J. G. WANG and R. RAJ, *J. Amer. Ceram. Soc.* **67** (1984) 399.
17. R. I. TODD, in "Superplasticity: 60 years after Pearson," edited by N. Ridley (The Institute of Materials, London, 1995) p. 33.
18. P. M. HAZZLEDINE and D. E. NEWBURY, in "Grain Boundary Structure and Properties," edited by G. A. Chadwick and D. A. Smith (Academic Press, London, 1976) p. 235.
19. A. P. SUTTON and R. W. BALLUFFI, "Interfaces in Crystalline Materials" (Clarendon Press, Oxford, 1995) p. 781.
20. A. G. EVANS, J. R. RICE and J. P. HIRTH, *J. Amer. Ceram. Soc.* **63** (1980) 368.
21. A. G. EVANS, *Acta Metall.* **28** (1980) 1155.
22. K. TSUKUMA and M. SHIMADA, *J. Mater. Sci. Lett.* **4** (1985) 857.
23. D. W. LIVESEY and N. RIDLEY, *Metal Sci.* **16** (1982) 563.
24. T. G. NIEH and J. WADSWORTH, in "Progress in Advanced Materials and Mechanics (ICAM'96)," edited by Wang Tzuchiang and Tsu-wei Chou (Peking University Press, Beijing, 1996) p. 423.
25. A. BRAVO-LEON, M. JIMENEZ-MELENDO and A. DOMINGUEZ-RODRIGUEZ, *Acta Metall. Mater.* **40** (1992) 2717.
26. S. L. HWANG and I.-W. CHEN, *J. Amer. Ceram. Soc.* **73** (1990) 3269.
27. D. HULL and D. E. RIMMER, *Phil. Mag.* **4** (1959) 673.
28. J. W. HANCOCK, *Metal. Sci.* **10** (1976) 319.
29. A. H. CHOKSHI and T. G. LANGDON, *Acta Metall.* **35** (1987) 1089.
30. J. PILLING and N. RIDLEY, *Res. Mechanica* **23** (1988) 31.
31. M. J. STOWELL, *Metal Sci.* **14** (1980) 267.
32. Z. X. GUO and N. RIDLEY, *Mater. Sci. Technol.* **6** (1990) 516.
33. T. G. LANGDON, in "Superplasticity: 60 years after Pearson," edited by N. Ridley (The Institute of Materials, London, 1995) p. 9.

Received 18 July 1997
and accepted 15 December 1998